Accepted Manuscript

Optimized design of Bézier surface through Bézier geodesic quadrilateral

Huogen Yang, Guozhao Wang

PII: S0377-0427(14)00290-8
DOI: http://dx.doi.org/10.1016/j.cam.2014.06.017
Reference: CAM 9714

To appear in: *Journal of Computational and Applied Mathematics*

Received date: 27 August 2013
Revised date: 23 March 2014

Please cite this article as: H. Yang, G. Wang, Optimized design of Bézier surface through Bézier geodesic quadrilateral, *Journal of Computational and Applied Mathematics* (2014), http://dx.doi.org/10.1016/j.cam.2014.06.017

Optimized design of Bézier surface through Bézier geodesic quadrilateral

Huogen Yang [a,b,*], Guozhao Wang[a]

[a] *Department of Mathematics, Zhejiang University, Hangzhou 310027, China*
[b] *Faculty of Science,Jiangxi University of Science and Technology , Ganzhou 341000, China*

Abstract

This paper studies constructing polynomial Bézier surface that interpolates a Bézier curvilinear quadrilateral as boundary geodesics. The construction consists of two parts. First, from the given corner data(i.e., position, tangent and curvature at the corner of each curve), four quintic Bézier curvilinear quadrilateral with minimum strain energy is constructed to satisfy the constraints of the crossing geodesics on a surface. Second, a polynomial Bézier surface of degree $(7, 7)$ is constructed to interpolate the quadrilateral as boundary geodesics of the constructed surface. We identify the precise degrees of freedom in terms of the control points. And the constructed surface that adheres to the NURBS standard and employs geometric shape handles can be readily incorporated into commercial CAD systems. The method is illustrated by several computational examples.

Key words: Bézier surface, interpolation, geodesic quadrilateral, optimized design

1. Introduction

The geodesic of the arbitrary two points on a surface is a locally length-minimizing curve [1]. Due to its intrinsic geometric feature, geodesic plays an important role in a diversity of applications, such as image processing and analysis [2, 3, 4], industrial designing and manufacturing [5, 6, 7], etc.

Surface construction via one or several given curves interpolation is a classic topic in the CAD & CAGD fields. In recent years, surface construction from one or several geodesic curves has attracted the attention from many researchers. And both independent and crossing geodesic curves have been considered. In the case of independent curves, several methods have been proposed for surface interpolating these curves as isoparametric geodesics [7, 8, 9, 10, 11, 12]. In the

*corresponding author
Email addresses: yanghuogen@126.com (Huogen Yang)
Tel/Fax:+86-0797-8312040 (Huogen Yang)

case of crossing curves, Hagen [13] developed a triangular interpolation scheme which results in a triangular surface with geodesic boundary curves. Farouki et al. identified the constraint conditions of the crossing geodesics on a surface [14], and from the given corner data, they also proposed to construct quadrilateral and triangular patches interpolating a geodesic quadrilateral [15] and triangle[16] by the Coons method, respectively. However, due to the restrictions of the crossing geodesic constraints and the Coons interpolation scheme, the degrees of the geodesic curves and the interpolation patch all are very high. For example with polynomial Bézier geodesic curves, the degree 7 was considered in [15], and each variable of the Coons interpolation surface patch is of degree 13. In modern CAD systems, high degree of the curve/surface may arouse inconvenience for curve/surface editing, and the probability of success of data exchange will be reduced between different systems. Thus, for the practical application, the immediate question is whether there are curve and surface with lower degree to satisfied the constraints of the geodesic quadrilateral interpolation.

Inspired by this, here we focus on the construction of polynomial Bézier surface with lower degree to interpolate Bézier curves as geodesic quadrilateral, and the constructed surface meets the requirements of the commercial CAD systems, such as the NURBS standard and the geometric shape handles[10], etc. To achieve this goal, we split the construction process into two parts. First, from the given corner data(position, tangent and curvature at the corner of each curve), we construct a polynomial Bézier curvilinear quadrilateral with minimum strain energy to satisfy the constraints required for the crossing geodesics on a surface. Then, a Bézier patch, whose control points are determined by two steps, is constructed to interpolate these curves as geodesic quadrilateral.

The paper is organized as follows. After introducing some notations and reviewing the constraint conditions for the crossing geodesics on a smooth surface in section 2. Section 3 identifies the constraint conditions for a quintic Bézier curvilinear quadrilateral to be the geodesic quadrilateral of a surface, and proposes a optimized geometric construction for quintic Bézier curvilinear quadrilateral which can be four boundary geodesics of a Bézier patch. Then in section 4, we describe in detail the construction of a Bézier patch to interpolate these curves as boundary geodesics. Finally, we draw our conclusions in Section 5.

2. Preliminaries

2.1. Notations

In the following discussion, all curves are free of inflection point, all surfaces are considered to be regular and oriented.

The inner product of two vectors $\boldsymbol{u}, \boldsymbol{v}$ is denoted by $< \boldsymbol{u}, \boldsymbol{v} >$. For linearly independent vectors $\boldsymbol{u}, \boldsymbol{v}$ and $\boldsymbol{n}$ such that $\boldsymbol{n} \perp \boldsymbol{u}$ and $\boldsymbol{n} \perp \boldsymbol{v}$, we denote by $(\boldsymbol{u}, \boldsymbol{v})_{\boldsymbol{n}}$ the oriented angle between $\boldsymbol{u}$ and $\boldsymbol{v}$ in the sense of $\boldsymbol{n}$, namely, $\sin(\boldsymbol{u}, \boldsymbol{v})_{\boldsymbol{n}} = \det(\frac{\boldsymbol{u}}{\|\boldsymbol{u}\|}, \frac{\boldsymbol{v}}{\|\boldsymbol{v}\|}, \frac{\boldsymbol{n}}{\|\boldsymbol{n}\|}), \cos(\boldsymbol{u}, \boldsymbol{v})_{\boldsymbol{n}} =< \frac{\boldsymbol{u}}{\|\boldsymbol{u}\|}, \frac{\boldsymbol{v}}{\|\boldsymbol{v}\|} >$.

For a space curve $\boldsymbol{r}(t)$, we denote by $\boldsymbol{e}(t), \boldsymbol{n}(t)$ and $\boldsymbol{b}(t)$ the tangent, principal normal and binormal vectors, by $k(t)$ and $\tau(t)$ the curvature and torsion of the curve at the point $\boldsymbol{r}(t)$, respectively. Namely,

$$\begin{aligned} &\boldsymbol{e}(t) = \frac{\boldsymbol{r}'(t)}{\|\boldsymbol{r}'(t)\|}, \quad \boldsymbol{b}(t) = \frac{\boldsymbol{r}'(t) \times \boldsymbol{r}''(t)}{\|\boldsymbol{r}'(t) \times \boldsymbol{r}''(t)\|}, \quad \boldsymbol{n}(t) = \boldsymbol{b}(t) \times \boldsymbol{e}(t), \\ &k(t) = \frac{\|\boldsymbol{r}'(t) \times \boldsymbol{r}''(t)\|}{\|\boldsymbol{r}'(t)\|^3}, \quad \tau(t) = \frac{det(\boldsymbol{r}'(t), \boldsymbol{r}''(t), \boldsymbol{r}'''(t))}{\|\boldsymbol{r}'(t) \times \boldsymbol{r}''(t)\|^2}. \end{aligned} \tag{1}$$

2.2. Constraints for geodesic boundaries crossing on a smooth surface

Consider, as illustrated in Fig.1, four regular curves $\boldsymbol{r}_1(u), \boldsymbol{r}_2(v), \boldsymbol{r}_3(u), \boldsymbol{r}_4(v)$ with $u, v \in [0, 1]$, such that $\boldsymbol{r}_1(0) = \boldsymbol{r}_2(0) = P_{00}, \boldsymbol{r}_1(1) = \boldsymbol{r}_4(0) = P_{10}, \boldsymbol{r}_2(1) = \boldsymbol{r}_3(0) = P_{01}, \boldsymbol{r}_3(1) = \boldsymbol{r}_4(1) = P_{11}$, Denote by $\boldsymbol{n}_i(j), k_i(j)$ and $\tau_i(j)(i = 1, \cdots, 4, j = 0, 1)$ the principal normal vectors, curvature and torsion at the two endpoints of the curves $\boldsymbol{r}_i$. Let $A_{00} = (\boldsymbol{r}_1'(0), \boldsymbol{r}_2'(0))_{\mathbf{N}(P_{00})}$, $A_{01} = (\boldsymbol{r}_3'(0), \boldsymbol{r}_2'(1))_{\mathbf{N}(P_{01})}$, $A_{10} = (\boldsymbol{r}_1'(1), \boldsymbol{r}_4'(0))_{\mathbf{N}(P_{10})}$, $A_{11} = (\boldsymbol{r}_3'(1), \boldsymbol{r}_4'(1))_{\mathbf{N}(P_{11})}$, $\mathbf{N}(P_{lj})$ are the unit normal vector of the interpolating surface at the corner $P_{lj}(l = 0, 1)$.

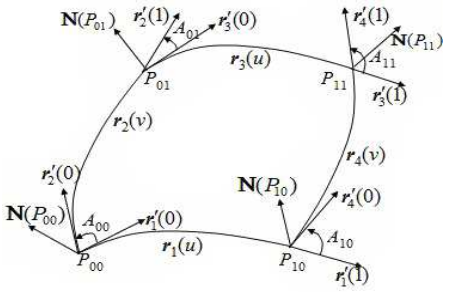

Figure 1: Patch boundaries and the vectors at the corners.

For the above four curves, Farouki et al. identified the conditions for them to constitute geodesic boundaries of a surface as follows.

Proposition 1. *(See [14]) If the four curves satisfy the following conditions:*
(C1) the osculating constraints;
(C2) the global normal orientation constraint;
(C3) geodesic crossing constraints at corners P_{lj}.
there exist a regular oriented surface $\boldsymbol{R}(u, v)$ interpolating these four curves in such a way that these curves are geodesics of the surface. Conversely, if any of the conditions(C1)-(C3) is not satisfied, such an interpolating surface can not be constructed.

For subsequent use, the three constraints of Proposition 1 listed as follows(see [14] for more details).

(C1) *Osculating constraints:* the principal normals of the boundary curves that meet at each corner must agree modulo sign.

$$\begin{aligned} &P_{00}: \sigma_1(0)\boldsymbol{n}_1(0) = \sigma_2(0)\boldsymbol{n}_2(0), \qquad &&P_{01}: \sigma_2(1)\boldsymbol{n}_2(1) = \sigma_3(0)\boldsymbol{n}_3(0), \\ &P_{10}: \sigma_1(1)\boldsymbol{n}_1(1) = \sigma_4(0)\boldsymbol{n}_4(0), \qquad &&P_{11}: \sigma_3(1)\boldsymbol{n}_3(1) = \sigma_4(1)\boldsymbol{n}_4(1). \end{aligned} \tag{2}$$

where $\sigma_i(j) \in \{-1, +1\}, i = 1, \cdots, 4, j = 0, 1$.

(C2) *Global normal orientation constraint:* Along the boundary curves, a continuous unit normal vector $\mathbf{N}$ of the interpolation surface must exist, such that $\mathbf{N} = \pm\boldsymbol{n}$($\boldsymbol{n}$ is the principal normal vector along the boundary curves).

(C3) *Corner geodesic crossing constraints:* At each corner, the curvature and torsion must satisfy

$$\begin{aligned} P_{00}: &\quad [\sigma_1(0)k_1(0) - \sigma_2(0)k_2(0)]\cos A_{00} + [\tau_1(0) + \tau_2(0)]\sin A_{00} = 0, \\ P_{01}: &\quad [\sigma_3(0)k_3(0) - \sigma_2(1)k_2(1)]\cos A_{01} + [\tau_3(0) + \tau_2(1)]\sin A_{01} = 0, \\ P_{11}: &\quad [\sigma_3(1)k_3(1) - \sigma_4(1)k_4(1)]\cos A_{11} + [\tau_3(1) + \tau_4(1)]\sin A_{11} = 0, \\ P_{10}: &\quad [\sigma_1(1)k_1(1) - \sigma_4(0)k_4(0)]\cos A_{10} + [\tau_1(1) + \tau_4(0)]\sin A_{10} = 0. \end{aligned} \tag{3}$$

3. Quintic Bézier curvilinear geodesic quadrilateral

In terms of the given corner data, in this section, we consider the constraints and construction for a quadrilateral, composed of four quintic polynomial Bézier curves with minimum strain energy, as boundary geodesics of a patch. Supposing the four curves defined as

$$\boldsymbol{r}_i(u) = \sum_{j=0}^{5} P_j^i B_{j,5}(u)(i = 1, 3) \quad \textit{and} \quad \boldsymbol{r}_i(v) = \sum_{j=0}^{5} P_j^i B_{j,5}(v)(i = 2, 4). \tag{4}$$

with $P_0^1 = P_0^2 = P_{00}, P_5^2 = P_0^3 = P_{01}, P_5^3 = P_5^4 = P_{11}, P_5^1 = P_0^4 = P_{10}$. And the strain energy of the four curves is defined as follows(see [17]).

$$\int_0^1 (\|\boldsymbol{r}_1''(u)\|^2 + \|\boldsymbol{r}_3''(u)\|^2)du + \int_0^1 (\|\boldsymbol{r}_2''(v)\|^2 + \|\boldsymbol{r}_4''(v)\|^2)dv. \tag{5}$$

3.1. Constraints for quintic Bézier curvilinear geodesic quadrilateral

(1) *Osculating constraints*

Consider the Osculating constraints at the corner P_{00}. Because the principal normal vector $\boldsymbol{n}_1(0)$ and $\boldsymbol{n}_2(0)$ are parallel with the unit normal vector $\mathbf{N}(P_{00}) = \frac{\boldsymbol{r}_1'(0)\times\boldsymbol{r}_2'(0)}{\|\boldsymbol{r}_1'(0)\times\boldsymbol{r}_2'(0)\|}$ of the interpolation surface at the corner P_{00}, the osculating plane Π_{01} of $\boldsymbol{r}_1(u)$ at the point P_{00} can be determined by $\boldsymbol{r}_1'(0)$ (parallel to $\overrightarrow{P_0^1P_1^1}$) and $\boldsymbol{r}_1'(0) \times \boldsymbol{r}_2'(0)$ (parallel to $\overrightarrow{P_0^1P_1^1} \times \overrightarrow{P_0^2P_1^2}$). Note that $\boldsymbol{r}_1'(0) \times \boldsymbol{r}_1''(0)$, namely, $\overrightarrow{P_0^1P_1^1} \times \overrightarrow{P_1^1P_2^1}$ is orthogonal to Π_{01} , so the control point P_2^1 must be located in the osculating plane Π_{01}. Similarly, the control point P_2^2 is located in the

osculating plane Π_{11} determined by $\boldsymbol{r}_2'(0)$ and $\boldsymbol{r}_1'(0) \times \boldsymbol{r}_2'(0)$ at the corner P_{00}. Then for all corners, we have

Remark 1. Osculating constraints imply that the control points P_2^i and P_3^i are located in the osculating plane of the curve $\boldsymbol{r}_i$ at the two end-points, respectively. And the osculating plane is determined by the tangent vector of the curve $\boldsymbol{r}_i$ and the normal vector of the interpolation surface at the end-point.

Furthermore, for the given corner data, we have

Theorem 1. *If the corner points, tangent and curvature at the corner of each curve are given, the control points P_2^i and P_3^i are located in the following two straight lines L_{0i} and L_{1i}, respectively.*

$$\begin{aligned} L_{0i}: &\quad \frac{x - x_{Q_0^i}}{X_{0i}} = \frac{y - y_{Q_0^i}}{Y_{0i}} = \frac{z - z_{Q_0^i}}{Z_{0i}}, \\ L_{1i}: &\quad \frac{x - x_{Q_1^i}}{X_{1i}} = \frac{y - y_{Q_1^i}}{Y_{1i}} = \frac{z - z_{Q_1^i}}{Z_{1i}}. \end{aligned} \tag{6}$$

where
$\overrightarrow{P_0^iP_1^i} = (X_{0i}, Y_{0i}, Z_{0i})$, $\overrightarrow{P_4^iP_5^i} = (X_{1i}, Y_{1i}, Z_{1i})$,
$Q_0^i = P_0^i + \sigma_i(0)\frac{5}{4}k_i(0)\|\overrightarrow{P_0^iP_1^i}\|^2\mathbf{N}(P_0^i) = (x_{Q_0^i}, y_{Q_0^i}, z_{Q_0^i})$,
$Q_1^i = P_5^i + \sigma_i(1)\frac{5}{4}k_i(1)\|\overrightarrow{P_4^iP_5^i}\|^2\mathbf{N}(P_5^i) = (x_{Q_1^i}, y_{Q_1^i}, z_{Q_1^i})$.

Proof. We shall give the proof only for the control point P_2^1 of the curve $\boldsymbol{r}_1(u)$. The proof for the other point P_2^i or P_3^i is similar.

Denote by d the distance from the point P_2^1 to the straight line $P_0^1P_1^1$. Using the curvature expression in (1), by direct calculation, we have

$$k_1(0) = \frac{4}{5}\frac{\|\overrightarrow{P_0^1P_1^1} \times \overrightarrow{P_0^1P_2^1}\|}{\|\overrightarrow{P_0^1P_1^1}\|^3} = \frac{4}{5}\frac{d}{\|\overrightarrow{P_0^1P_1^1}\|^2}.$$

Then the distance d can be expressed as

$$d = \frac{5}{4}k_1(0)\|\overrightarrow{P_0^1P_1^1}\|^2. \tag{7}$$

Expression (7) indicates that d is a fixed value when the corner data are given. Namely, the control point P_2^1 is always located in a straight line L which parallels to the straight line $P_0^1P_1^1$, and the distance between the two straight lines is d(see Fig.2).

Let

$$Q_0^1 = P_0^1 + \sigma_1(0)d\mathbf{N}(P_0^1). \tag{8}$$

From (7) and (8), we can find the point Q_0^1 is located in the osculating plane Π_{01}, the points Q_0^1 and P_2^1 are located at the same side of the straight line $P_0^1P_1^1$, and the distance from the point Q_0^1 to the straight line $P_0^1P_1^1$ is d. So the straight line L also passes through the point $Q_0^1 = (x_{Q_0^1}, y_{Q_0^1}, z_{Q_0^1})$. Thus the equation of the straight line L can be expressed as

$$\frac{x - x_{Q_0^1}}{X_{01}} = \frac{y - y_{Q_0^1}}{Y_{01}} = \frac{z - z_{Q_0^1}}{Z_{01}}.$$

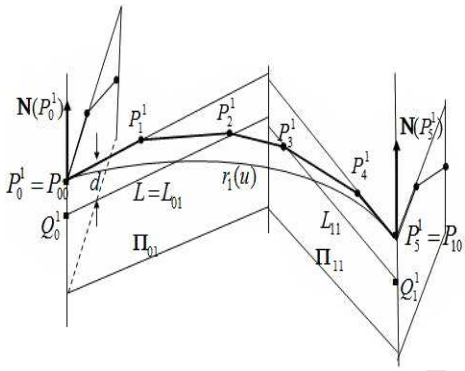

Figure 2: The choice of the control point P_2^1.

This is the equation of straight line L_{01} of equations (6). □

(2) *Global normal orientation constraint*

Due to the interpolating surface orientation and the curve $\boldsymbol{r}_i$ without inflection point, both the unit normal $\mathbf{N}$ of the surface and the principal normal $\boldsymbol{n}$ of each curve are globally continuous. Then the global normal orientation constraint shows such a fact: For $\mathbf{N}=\boldsymbol{n}$ or $\mathbf{N}=-\boldsymbol{n}$, only one of the two holds along each boundary curve. Therefore, the sudden reversal of the principal normal can only occur at four corners, and the number of reversals is even. Namely,

$$\prod_{i,j}\sigma_i(j)=1, \quad (i=1,\cdots,4, j=0,1). \tag{9}$$

(3) *Corner geodesic crossing constraints*

Let $P_2^i=(x_{P_2^i},y_{P_2^i},z_{P_2^i})$, $P_3^i=(x_{P_3^i},y_{P_3^i},z_{P_3^i})$,$\overrightarrow{P_0^iP_1^i}\times\overrightarrow{P_0^iQ_0^i}=(x_{0i},y_{0i},z_{0i})$ and $\overrightarrow{P_5^iQ_1^i}\times\overrightarrow{P_4^iP_5^i}=(x_{1i},y_{1i},z_{1i})$, We have

Theorem 2. *Corner geodesic crossing constraints (3) is equivalent to*

$$\begin{cases} a_{01}x_{P_3^1}+a_{02}x_{P_3^2}=\frac{125}{48}[\sigma_2(0)k_2(0)-\sigma_1(0)k_1(0)]\cot A_{00}+b_{01}+b_{02},\\ a_{03}x_{P_3^3}+a_{12}x_{P_2^2}=\frac{125}{48}[\sigma_2(1)k_2(1)-\sigma_3(0)k_3(0)]\cot A_{01}+b_{03}+b_{12},\\ a_{13}x_{P_2^3}+a_{14}x_{P_2^4}=\frac{125}{48}[\sigma_4(1)k_4(1)-\sigma_3(1)k_3(1)]\cot A_{11}+b_{13}+b_{14},\\ a_{11}x_{P_2^1}+a_{04}x_{P_3^4}=\frac{125}{48}[\sigma_4(0)k_4(0)-\sigma_1(1)k_1(1)]\cot A_{10}+b_{11}+b_{04}. \end{cases} \tag{10}$$

Where

$$a_{0i}=\frac{1}{k_i^2(0)\|\overrightarrow{P_0^iP_1^i}\|^6}(x_{0i}+y_{0i}\frac{Y_{1i}}{X_{1i}}+z_{0i}\frac{Z_{1i}}{X_{1i}}),$$

$$a_{1i}=\frac{1}{k_i^2(1)\|\overrightarrow{P_4^iP_5^i}\|^6}(x_{1i}+y_{1i}\frac{Y_{0i}}{X_{0i}}+z_{1i}\frac{Z_{0i}}{X_{0i}}),$$

$$b_{0i}=\frac{1}{k_i^2(0)\|\overrightarrow{P_0^iP_1^i}\|^6}[x_{0i}x_{P_0^i}+y_{0i}(\frac{Y_{1i}}{X_{1i}}x_{Q_1^i}-y_{Q_1^i}+y_{P_0^i})+z_{0i}(\frac{Z_{1i}}{X_{1i}}x_{Q_1^i}-z_{Q_1^i}+z_{P_0^i})],$$

$$b_{1i}=\frac{1}{k_i^2(1)\|\overrightarrow{P_4^iP_5^i}\|^6}[x_{1i}x_{P_5^i}+y_{1i}(\frac{Y_{0i}}{X_{0i}}x_{Q_0^i}-y_{Q_0^i}+y_{P_5^i})+z_{1i}(\frac{Z_{0i}}{X_{0i}}x_{Q_0^i}-z_{Q_0^i}+z_{P_5^i})].$$

Proof. Notice that,

$$\overrightarrow{P_0^iP_1^i} \times \overrightarrow{P_0^iP_2^i} = \overrightarrow{P_0^iP_1^i} \times \overrightarrow{P_0^iQ_0^i}, \quad \|\overrightarrow{P_0^iP_1^i} \times \overrightarrow{P_0^iP_2^i}\|^2 = \frac{25}{16}k_i^2(0)|\overrightarrow{P_0^iP_1^i}\|^6,$$
$$\overrightarrow{P_4^iP_5^i} \times \overrightarrow{P_3^iP_5^i} = \overrightarrow{P_5^iQ_1^i} \times \overrightarrow{P_4^iP_5^i}, \quad \|\overrightarrow{P_4^iP_5^i} \times \overrightarrow{P_3^iP_5^i}\|^2 = \frac{25}{16}k_i^2(1)|\overrightarrow{P_4^iP_5^i}\|^6.$$

Substituting these expressions into the torsion expression in (1), we have

$$\tau_i(0) = \frac{48\det(\overrightarrow{P_0^iP_1^i}, \overrightarrow{P_0^iQ_0^i}, \overrightarrow{P_0^iP_3^i})}{125k_i^2(0)|\overrightarrow{P_0^iP_1^i}\|^6}, \quad \tau_i(1) = \frac{48\det(\overrightarrow{P_4^iP_5^i}, \overrightarrow{P_5^iQ_1^i}, \overrightarrow{P_2^iP_5^i})}{125k_i^2(1)|\overrightarrow{P_4^iP_5^i}\|^6}. \quad (11)$$

From (6), the torsions $\tau_i(0)$ and $\tau_i(1)$ are expressed by $x_{P_3^i}$ and $x_{P_2^i}$. Then substituting (11) into constraint (3), by direct calculation, equation (10) is obtained. □

According to Theorem 1, the control points P_2^i and P_3^i can be determined by their x-coordinate $x_{P_2^i}$ and $x_{P_3^i}(i = 1, 2, 3, 4)$. Considering the four curves with minimum strain energy and the constraint (10) on $x_{P_2^i}$ and $x_{P_3^i}$, then, we can determine $x_{P_2^i}$ and $x_{P_3^i}$ by minimizing formula (5) with the constraint (10).

3.2. Construction of quintic Bézier curvilinear geodesic quadrilateral

According to the analysis of section 3.1, we now propose a optimized geometric construction for a quadrilateral, composed of four quintic Bézier curves with the constraints of the surface geodesic quadrilateral. The construction consists of the following six steps.

(1) *From the corner data, the control points P_0^i, P_1^i and P_4^i, P_5^i can be determined.*

(2) *An orientation unit normal vector $\boldsymbol{N}(P_{lj})$ of the interpolation surface is assigned at each corner, defining the orientation of the surface.*

(3) *A sequence of signs $\sigma_i(0)$ and $\sigma_i(1)$ is chosen, compatible with the global normal orientation constraint (9).*

(4) *According to equations (6), the straight line L_{0i} and L_{1i} are determined.*

(5) *Determining $x_{P_2^i}$ and $x_{P_3^i}$ by minimizing formula (5) with the constraint (10), thus the corner geodesic crossing constraints (3) are satisfied.*

(6) *From equations (6), $y_{P_2^i}, z_{P_2^i}, y_{P_3^i}$ and $z_{P_3^i}$ are obtained, and the control points P_2^i and P_3^i are determined.*

Fig.3 shows two examples of the quadrilateral with control polygon, constructed in the above manner.

4. Four-sided geodesic Bézier interpolation

we now construct a Bézier patch that interpolates the above constructed curves as geodesic quadrilateral. For simplification, the parametric variables u and v all are denoted by t in this section.

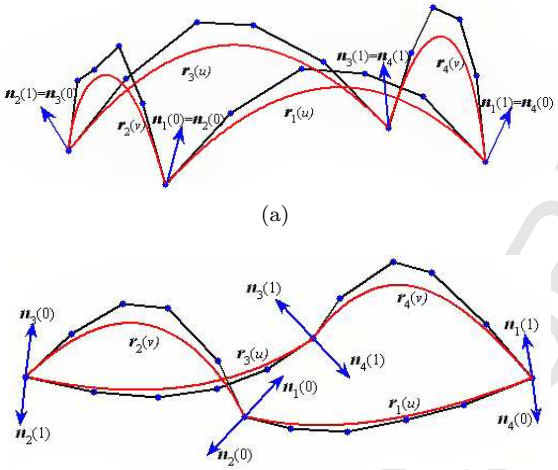

Figure 3: The constructed quintic Bézier curvilinear quadrilateral. (a)Continuous principal normal along the boundary. (b)Four reversals of principal normal occur at the four corners.

4.1. Compatibility of interpolation conditions

Along the geodesic boundaries $\boldsymbol{r}_i(t)$, the transverse tangent vector $\boldsymbol{D}_i(t)$ of the interpolation patch is coplanar with the vector $\boldsymbol{r}_i'(t)$ and $\boldsymbol{r}_i'(t) \times \boldsymbol{r}_i''(t)$, so there exist scalar functions $\alpha_i(t)$ and $\beta_i(t)$ such that

$$\boldsymbol{D}_i(t) = \alpha_i(t)\boldsymbol{r}_i'(t) + \beta_i(t)\boldsymbol{r}_i'(t) \times \boldsymbol{r}_i''(t), \qquad t \in [0,1]. \tag{12}$$

Due to vanishing leading, the actual degree of the cross product $\boldsymbol{r}_i'(t) \times \boldsymbol{r}_i''(t)$ is of 6. Taking the corner compatibility of interpolation condition (12) at the corner and the degree of $\boldsymbol{D}_i(t)$ into consideration, we choose $\alpha_i(t) = \sum_{j=0}^{3} a_j^i B_{j,3}(t)$ and $\beta_i(t) = \sum_{j=0}^{1} b_j^i B_{j,1}(t)$. They are Bézier functions of degree 3 and 1 with the coefficients a_j^i and b_j^i, respectively.

The interpolation condition (12) must satisfy the compatibility conditions at each corner, which constrains the choice of the coefficients a_j^i and b_j^i. Consider, for example, the curve $\boldsymbol{r}_1(t)$ at the corner P_0^1 and P_5^1 .

(1) Compatibility of tangent vector

As the transverse tangent vector $\boldsymbol{D}_1(t)$ must interpolate the tangent vector of the curve $\boldsymbol{r}_2(t)$ and $\boldsymbol{r}_4(t)$ at the corner P_0^1 and P_5^1, respectively. Let $i = 1, t = 0$ in (12), we have

$$a_0^1 \overrightarrow{P_0^1 P_1^1} + 20 b_0^1 \overrightarrow{P_0^1 P_1^1} \times \overrightarrow{P_0^1 P_2^1} = \overrightarrow{P_0^2 P_1^2}. \tag{13}$$

Because $\boldsymbol{r}_1'(0)$, $\boldsymbol{r}_2'(0)$ and $\boldsymbol{r}_1'(0) \times \boldsymbol{r}_1''(0)$ are coplanar, equation (13) admits so-

lutions as

$$a_0^1 = \frac{< \overrightarrow{P_0^1P_1^1}, \overrightarrow{P_0^2P_1^2} >}{\|\overrightarrow{P_0^1P_1^1}\|^2}, \qquad b_0^1 = \frac{\det(\overrightarrow{P_0^1P_1^1}, \overrightarrow{P_0^1P_2^1}, \overrightarrow{P_0^2P_1^2})}{20\|\overrightarrow{P_0^1P_1^1} \times \overrightarrow{P_0^1P_2^1}\|^2}. \tag{14}$$

Let $i = 1, t = 1$ in (12), in the same way, a_3^1 and b_1^1 are determined as follows.

$$a_3^1 = \frac{< \overrightarrow{P_4^1P_5^1}, \overrightarrow{P_0^4P_1^4} >}{\|\overrightarrow{P_4^1P_5^1}\|^2}, \qquad b_1^1 = \frac{\det(\overrightarrow{P_3^1P_5^1}, \overrightarrow{P_4^1P_5^1}, \overrightarrow{P_0^4P_1^4})}{20\|\overrightarrow{P_3^1P_5^1} \times \overrightarrow{P_4^1P_5^1}\|^2}.$$

Similarly solutions for $i = 2, 3, 4$ can be obtained, thus the first and last coefficients of $\alpha_i(t)$ and all the coefficients of $\beta_i(t)$ are determined.

(2) Compatibility of twist vector

Denote by $\boldsymbol{R}(u, v)$ the interpolation surface. Then, $\boldsymbol{D}_1(u) = \boldsymbol{R}_v(u, 0)$, $\boldsymbol{D}_2(v) = \boldsymbol{R}_u(0, v)$. At the corner P_0^1, differentiate $\boldsymbol{D}_1(u)$ and $\boldsymbol{D}_2(v)$, and set $u = 0$ and $v = 0$, we have

$$\boldsymbol{D}_1'(0) = \boldsymbol{R}_{u,v}(0, 0) = \boldsymbol{D}_2'(0). \tag{15}$$

To compare $\boldsymbol{D}_1'(0)$ and $\boldsymbol{D}_2'(0)$, we consider their projections on the three linearly-independent vectors $\boldsymbol{r}_1'(0), \boldsymbol{r}_2'(0)$ and unit normal $\mathbf{N}(P_0^1)$. Notice that

$$\mathbf{N}(P_0^1) = \sigma_1(0)\frac{(\boldsymbol{r}_1'(0) \times \boldsymbol{r}_1''(0)) \times \boldsymbol{r}_1'(0)}{\|(\boldsymbol{r}_1'(0) \times \boldsymbol{r}_1''(0)) \times \boldsymbol{r}_1'(0)\|} = \sigma_2(0)\frac{(\boldsymbol{r}_2'(0) \times \boldsymbol{r}_2''(0)) \times \boldsymbol{r}_2'(0)}{\|(\boldsymbol{r}_2'(0) \times \boldsymbol{r}_2''(0)) \times \boldsymbol{r}_2'(0)\|},$$
$$\sigma_1(0) = \frac{\|\boldsymbol{r}_1'(0) \times \boldsymbol{r}_2'(0)\|\|\boldsymbol{r}_1'(0) \times \boldsymbol{r}_1''(0)\|}{\|\boldsymbol{r}_1'(0)\| \det(\boldsymbol{r}_1'(0), \boldsymbol{r}_2'(0), \boldsymbol{r}_1''(0))}, \sigma_2(0) = \frac{\|\boldsymbol{r}_1'(0) \times \boldsymbol{r}_2'(0)\|\|\boldsymbol{r}_2'(0) \times \boldsymbol{r}_2''(0)\|}{\|\boldsymbol{r}_2'(0)\| \det(\boldsymbol{r}_2'(0), \boldsymbol{r}_2''(0), \boldsymbol{r}_1'(0))}.$$

Utilizing the curvature and torsion expressions in (1), (14) together with the identity $(\boldsymbol{u} \times \boldsymbol{v}) \times \boldsymbol{w} =< \boldsymbol{u}, \boldsymbol{w} > \boldsymbol{v} - < \boldsymbol{v}, \boldsymbol{w} > \boldsymbol{u}$, by calculation, we have

- Projection on $\mathbf{N}(P_0^1)$

$$< \boldsymbol{D}_1'(0), \mathbf{N}(P_0^1) >= \|\boldsymbol{r}_1'(0)\|\|\boldsymbol{r}_2'(0)\|[\sigma_1(0)k_1(0)\cos A_{00} + \tau_1(0)\sin A_{00}],$$
$$< \boldsymbol{D}_2'(0), \mathbf{N}(P_0^1) >= \|\boldsymbol{r}_1'(0)\|\|\boldsymbol{r}_2'(0)\|[\sigma_2(0)k_2(0)\cos A_{00} - \tau_2(0)\sin A_{00}].$$

As the corner geodesic crossing constraint is satisfied, $< \boldsymbol{D}_1'(0), \mathbf{N}(P_0^1) >=< \boldsymbol{D}_2'(0), \mathbf{N}(P_0^1) >$ holds naturally.

- Projection on $\boldsymbol{r}_1'(0)$

$$< \boldsymbol{D}_1'(0), \boldsymbol{r}_1'(0) >= 75(\|\overrightarrow{P_0^1P_1^1}\|^2 a_1^1 + c),$$
$$< \boldsymbol{D}_2'(0), \boldsymbol{r}_1'(0) >= 75(< \overrightarrow{P_0^1P_1^1}, \overrightarrow{P_0^2P_1^2} > a_1^2 + d).$$

Where $c = \frac{4a_0^1}{3} < \overrightarrow{P_0^1P_1^1}, \overrightarrow{P_0^1P_2^1} > -\frac{11a_0^1}{3}\|\overrightarrow{P_0^1P_1^1}\|^2$,
$d = \frac{4a_0^2}{3} < \overrightarrow{P_0^1P_1^1}, \overrightarrow{P_0^2P_2^2} > -\frac{11a_0^2}{3} < \overrightarrow{P_0^1P_1^1}, \overrightarrow{P_0^2P_1^2} > +[\frac{20(b_1^2 - b_0^2)}{3} - 60b_0^2] \cdot$
$\det(\overrightarrow{P_0^2P_1^2}, \overrightarrow{P_0^2P_2^2}, \overrightarrow{P_0^1P_1^1}) + 20b_0^2 \det(\overrightarrow{P_0^2P_1^2}, \overrightarrow{P_0^2P_3^2}, \overrightarrow{P_0^1P_1^1})$.

• Projection on $\boldsymbol{r}_2'(0)$

$$< \boldsymbol{D}_1'(0), \boldsymbol{r}_2'(0) >= 75(< \overrightarrow{P_0^1P_1^1}, \overrightarrow{P_0^2P_1^2} > a_1^1 + e),$$
$$< \boldsymbol{D}_2'(0), \boldsymbol{r}_2'(0) >= 75(\|\overrightarrow{P_0^2P_1^2}\|^2 a_1^2 + f).$$

Where e can be obtained with the superscript 1 and 2 of d replaced by 2 and 1, f can be obtained with the superscript 1 of c replaced by 2.

Thus, $\boldsymbol{D}_1'(0) = \boldsymbol{D}_2'(0)$ holds if and only if the following linear system of equations admit solutions

$$\begin{cases} \|\overrightarrow{P_0^1P_1^1}\|^2 a_1^1 - < \overrightarrow{P_0^1P_1^1}, \overrightarrow{P_0^2P_1^2} > a_1^2 = d - c, \\ < \overrightarrow{P_0^1P_1^1}, \overrightarrow{P_0^2P_1^2} > a_1^1 - \|\overrightarrow{P_0^2P_1^2}\|^2 a_1^2 = f - e. \end{cases} \tag{16}$$

In general, $\overrightarrow{P_0^1P_1^1}$ and $\overrightarrow{P_0^2P_1^2}$ are linearly-independent, so the solutions of equation (16) are unique. Similar equations will come up at the other three corners, and the coefficients a_1^i and $a_2^i (i = 1, 2, 3, 4)$ can be obtained from these equations.

4.2. Bézier expression of the interpolation patch

In order to express the interpolation surface as Bézier form, firstly, the transverse tangent vector function $\boldsymbol{D}_i(t)$ should be expressed as Bézier form.

Let $\Delta P_{j_1}^i = 5(P_{j_1+1}^i - P_{j_1}^i)(j_1 = 0, 1, \cdots, 4)$, $\Delta^2 P_{j_2}^i = 4(\Delta P_{j_2+1}^i - \Delta P_{j_2}^i)(j_2 = 0, 1, 2, 3)$. Notice that $\boldsymbol{r}_i'(t) \times \boldsymbol{r}_i''(t)$ is degree 6 Bézier curve, that is,

$$\boldsymbol{r}_i'(t) \times \boldsymbol{r}_i''(t) = \sum_{j_3=0}^{7} \overline{H}_{j_3}^i B_{j_3,7}(t) = \sum_{j_4=0}^{6} H_{j_4}^i B_{j_4,6}(t). \tag{17}$$

where

$$\overline{H}_{j_3}^i = \frac{1}{\binom{7}{j_3}} \sum_{0 \le j_1 \le 4}^{j_1+j_2=j_3} \sum_{0 \le j_2 \le 3} \binom{4}{j_1}\binom{3}{j_2} \Delta P_{j_1}^i \times \Delta^2 P_{j_2}^i,$$

$$H_{j_4}^i = \frac{7}{7 - j_4}(\overline{H}_{j_4}^i - \frac{j_4}{7} H_{j_4-1}^i), \quad H_{-1}^i = 0.$$

From (17)and (12), the transverse tangent vector $\boldsymbol{D}_i(t)$ can be expressed as following Bézier form.

$$\boldsymbol{D}_i(t) = \sum_{k=0}^{7} (F_k^i + G_k^i) B_{k,7}(t), \quad (i = 1, 2, 3, 4). \tag{18}$$

Where

$$F_k^i = \frac{1}{\binom{7}{k}} \sum_{0 \le j \le 3}^{j+j_1=k} \sum_{0 \le j_1 \le 4} \binom{3}{j}\binom{4}{j_1} a_j^i \times \Delta P_{j_1}^i,$$

$$G_k^i = \frac{k b_1^i}{7} H_{k-1}^i + (1 - \frac{k}{7}) b_0^i H_k^i, \quad H_7^i = 0.$$

Because the transverse tangent vector $\boldsymbol{D}_i(t)$ is of degree 7, we can define a interpolation Bézier patch with degree $(7,7)$ as

$$\boldsymbol{R}(u,v)=\sum_{i=0}^{7}\sum_{j=0}^{7}D_{ij}B_{i,7}(u)B_{j,7}(v). \tag{19}$$

Using the degree elevation formula of Bézier curve, we rewrite $\boldsymbol{r}_i(t)$ as

$$\boldsymbol{r}_i(t)=\sum_{k=0}^{7}\boldsymbol{d}_k^i B_{k,7}(t).$$

where $\boldsymbol{d}_k^i=(1-\frac{k}{7})\overline{\boldsymbol{d}}_k^i+\frac{k}{7}\overline{\boldsymbol{d}}_{k-1}^i,\quad \overline{\boldsymbol{d}}_{-1}^i=\overline{\boldsymbol{d}}_7^i=0,$
$\overline{\boldsymbol{d}}_j^i=(1-\frac{j}{6})\boldsymbol{P}_j^i+\frac{j}{6}\boldsymbol{P}_{j-1}^i(j=0,1,\cdots,6),\quad \boldsymbol{P}_{-1}^i=\boldsymbol{P}_6^i=0.$
It is obvious that

$$\begin{cases} D_{i0}=\boldsymbol{d}_i^1, & D_{i,7}=\boldsymbol{d}_i^3, & (i=0,1,\cdots,7),\\ D_{0j}=\boldsymbol{d}_j^2, & D_{7,j}=\boldsymbol{d}_j^4, & (j=0,1,\cdots,7). \end{cases} \tag{20}$$

By calculating directly the transverse tangent vector of $\boldsymbol{R}(u,v)$, and using (18) and (20), we have

$$\begin{cases} D_{i1}=\boldsymbol{d}_i^1+\frac{1}{7}(F_i^1+G_i^1),\\ D_{1j}=\boldsymbol{d}_j^2+\frac{1}{7}(F_j^2+G_j^2), & (i=1,\cdots,6),\\ D_{i6}=\boldsymbol{d}_i^3-\frac{1}{7}(F_i^3+G_i^3), & (j=1,\cdots,6).\\ D_{6j}=\boldsymbol{d}_j^4-\frac{1}{7}(F_j^4+G_j^4), \end{cases} \tag{21}$$

Notice that, the twist points of $\boldsymbol{R}(u,v)$ are calculated twice in (21), but they are compatible when relation (15) holds.

We can now state the following result.

Theorem 3. *For the quintic Bézier curvilinear quadrilateral constructed by the method of section 3.2, if the control points of boundary curves and next to boundary curves of the surface (19) satisfy Formulas (20) and (21), the surface (19) interpolates the quadrilateral as boundary geodesics quadrilateral.*

Theorem 3 indicates that, along each boundary curve, there are two lines of control points related with the geodesic interpolation condition. One line of control points is inherited from the boundary geodesic, the other line of control points is adjacent to those of the boundary curve. The remaining inner control points are free. In order to obtain a fair interpolation surface, we choose the free control points by minimizing the following thin plate spline energy.

$$\min_{D_{ij}}[\int_0^1\int_0^1(\|\boldsymbol{R}_{uu}(u,v)\|^2+2\|\boldsymbol{R}_{uv}(u,v)\|^2+\|\boldsymbol{R}_{vv}(u,v)\|^2)dudv].$$

Let $\frac{\partial E}{\partial D_{ij}}=0(i,j=2,\ldots,5)$, we have

$$\sum_{0\le k\le 7,k\ne i,}\ \sum_{0\le l\le 7,l\ne j}D_{kl}M_{i,j,k,l}+D_{ij}M_{i,j,i,j}=0. \tag{22}$$

where

$$M_{i,j,k,l} = \int_0^1 \int_0^1 \begin{pmatrix} B''_{i,7}(u)B_{j,7}(v)B''_{k,7}(u)B_{l,7}(v) \\ +2B'_{i,7}(u)B'_{j,7}(v)B'_{k,7}(u)B'_{l,7}(v) \\ +B_{i,7}(u)B''_{j,7}(v)B_{k,7}(u)B''_{l,7}(v) \end{pmatrix} dudv.$$

The free control points $D_{ij}(i, j = 2, \ldots, 5)$ can be obtained by solving the linear equation (22).

Based on the above analysis, for a Bézier curvilinear quadrilateral constructed by the method in section 3.2, the Bézier patch which interpolates these curves as geodesic quadrilateral can be constructed by the following steps.

(1) *According to the compatibility of the tangent and twist vector at the corners in Section 4.1, $\alpha_i(t)$ and $\beta_i(t)$ are determined.*

(2) *From formula (18), we can calculate the control points of the transverse tangent vector function $\boldsymbol{D}_i(t)$.*

(3) *The control points of the interpolation patch, which are related with the geodesic interpolation condition, are calculated by formulas (20) and (21).*

(4) *The remaining control points of the interpolation patch are obtained by solving linear equation (22).*

Fig.4 and Fig.5 show two Bézier surfaces with degree $(7, 7)$ interpolating the constructed quadrilaterals(Fig.3(a),(b)) as geodesic quadrilateral, respectively.

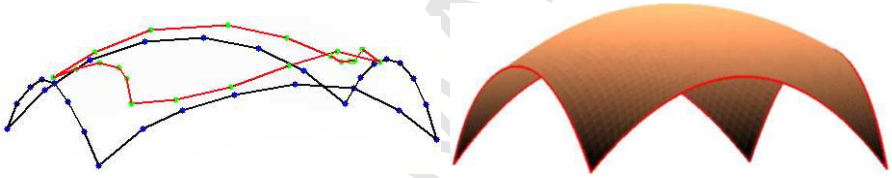

(a) (b)

Figure 4: (a)The Control points related with geodesic interpolation condition. (b)interpolation surface.

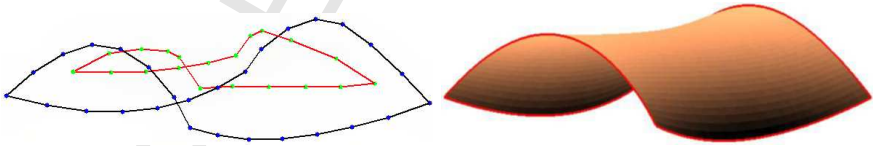

(a) (b)

Figure 5: (a)The Control points related with geodesic interpolation condition. (b)interpolation surface.

5. Conclusion

In this paper, we identify the constraint conditions for quintic polynomial Bézier curvilinear quadrilateral to constitute the boundary geodesics of a sur-

face, and propose a optimized geometric method to construct a quintic Bézier curvilinear quadrilateral satisfying these constraint conditions. For the constructed quadrilateral, a tensor-product Bézier surface of degree $(7, 7)$ can be constructed to interpolate these curves as geodesic quadrilateral. The scheme incurs the free control points, which can be used to smooth the interpolation surface. The interpolation surface patch adheres to the Bézier form and employs geometric shape handles, such as control points, which is compatible with commercial CAD systems.

Acknowledgements

The authors are very grateful to the referees for their helpful suggestions and comments. This work is supported by the National Natural Science Foundation of China (Grants No.61272300, No.60933008).

References

[1] M.P. Do Carmo, Differential geometry of curve and surfaces, Englewood Cliffs: Prentice Hall,1976.

[2] C.Bennis, J.M. Vézien, G.Iglésias, Piecewise surface flattening for non-distorted texture mapping, Computer Graphics 25(4)(1991)237-246.

[3] R.Kimmel, Intrinsic scale space for images on surfaces: the geodesic curvature flow, Graphical Models Image Process 59(5)(1997)365-372.

[4] R. Kimmel, R. Malladi, N. Sochen, Images as embedded maps and minimal surfaces: movies, color, texture, and volumetric medical images, International Journal of Computer Vision 39(2)(2000)111-129.

[5] C.L. Tucker III, Forming of advanced composites, in: T.G.Gutowski(Ed.), Advanced Composites Manufacturing, Wiley, New York, 1997,pp.297-372.

[6] R.J. Haw, An application of geodesic curves to sail design, Computer Graphics Forum 4(2)(1985)137-139.

[7] G.J. Wang, K.Tang, C.L.Tai, Parametric representation of a surface pencil with a common spatial geodesic, Computer-Aided Design 36(5)(2004)447-459.

[8] N.Sprynski, N.Szafran, B. Lacolle, L. Biard, Surface reconstruction via geodesic interpolation, Computer-Aided Design 40(4)(2008)480-492.

[9] M.Paluszny, Cubic polynomial patches through geodesics, Computer-Aided Design 40(1)(2008)56-61.

[10] J. Sánchez-Reyes, R. Dorado, Constrained design of polynomial surfaces from geodesic curves, Computer-Aided Design 40(1)(2008)49-55.

[11] C.Y. Li, R.H.Wang, C.G. Zhu, Designing and G^1 connection of developable surfaces through Bézier geodesics, Applied Mathematics and Computation 218(2011)3199-3208.

[12] C.Y. Li, R.H.Wang, C.G. Zhu, Designing approximation minimal parametric surfaces with geodesics, Applied Mathematical modelling 37(2013)6415-6424.

[13] H. Hagen, Geometric surface patches without twist constraints, Computer Aided Geometric Design 3(3)(1986)179-184.

[14] R.T. Farouki, N. Szafran, L. Biard, Existence conditions for Coons patches interpolating geodesic boundary curves, Computer Aided Geometric Design 26(5)(2009)599-614.

[15] R.T. Farouki, N. Szafran, L. Biard, Construction of Bézier surface patches with Bézier curves as geodesic boundaries, Computer-Aided Design 41(11)(2009)772-781.

[16] R.T. Farouki, N. Szafran, L. Biard, Construction and smoothing of triangular Coons patches with geodesic boundary curves, Computer Aided Geometric Design 27(4)(2010)301-312.

[17] J.H. Yong, F.H. Cheng, Geometric Hermite curves with minimum strain energy, Computer Aided Geometric Design 21(3)(2004)281-301.

Highlights

- A optimized geometric construction method for Bézier geodesic quadrilateral.
- A practical construction scheme for surface interpolating geodesic quadrilateral.
- We identify the precise degrees of freedom in terms of control points.
- The constructed surface and geodesics with low degree.